Zeolite Structure

A Zeolite Structure (ITQ-13) with Three Sets of Medium-Pore Crossing Channels Formed by 9- and 10-Rings**

Avelino Corma, Marta Puche, Fernando Rey, Gopinathan Sankar, and Simon J. Teat*

ZSM-5 (MFI code)[1] is a medium-pore zeolite that has 10-ring channels with pore diameters of 5.1 × 5.5 and 5.3 × 5.6 Å, and has been a very successful zeolite for shape-selective catalysis[2–4] that has found many industrial applications.

By considering the structure of ZSM-5 and the catalytic results obtained in the fields of oil refining and petrochemistry,[2–4] one could intuitively predict that a medium-pore zeolite with intersecting channels and pore dimensions that are slightly smaller than those of ZSM-5 should enhance the possibilities for shape-selective catalysis in the fields of fluid catalytic cracking (FCC) additives, catalytic dewaxing, toluene disproportionation, alkylation of aromatics, isomerization of alkylaromatics, and so forth.

Herein, we will describe such a zeolite structure (ITQ-13), which exhibits three sets of intercrossed medium-pore channels; a 9-ring channel, with a pore aperture of 4.0 × 4.9 Å, runs parallel to the crystallographic *a* axis, a 10-ring channel system (4.8 × 5.7 Å) runs parallel to the *c* axis, and another 10-ring set of channels (4.7 × 5.1 Å) runs parallel to the *b* axis.

Although it was not possible to determine the structure from powder diffraction alone, a preliminary powder diffraction study revealed the unit cell to be orthorhombic, with cell parameters of $a = 12.5$, $b = 11.3$ and $c = 21.9$ Å, which indicated that ITQ-13 is a unique microporous zeolitic material. With the advent of microdiffraction, we are now able to collect good-quality single-crystal data using a crystal with dimensions of 40 × 30 × 20 μm, to successfully solve the structure by direct methods. The Amm2 space group was confirmed by comparing the simulated powder X-ray diffraction (XRD) pattern using the single-crystal data, and the high-resolution XRD pattern recorded from the same powdered sample. Both analyses suggest a single-phase material with a unique structure. By using the coordinates of the tetrahedral cations (T-atoms), we calculated the coordination sequence and the vertex indexes (see Supporting Information),[5] which prove without doubt that the structure of ITQ-13 corresponds to a new zeolite topology.

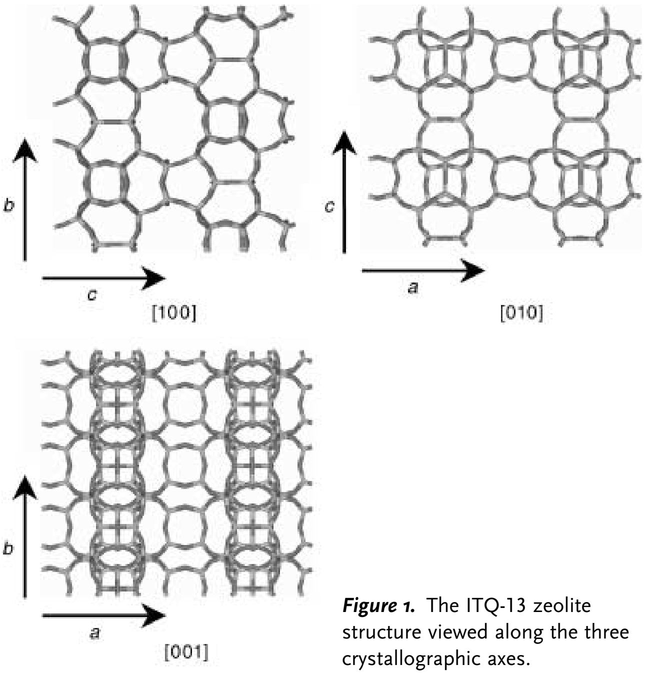

Figure 1. The ITQ-13 zeolite structure viewed along the three crystallographic axes.

The framework structure of the ITQ-13 zeolite along the three crystallographic axes is presented in Figure 1, and provides an illustration of the pore channels. The most striking feature is the three-dimensional connectivity of this medium-pore system, with three channels running parallel to the *a*, *b*, and *c* crystallographic axes. One set of channels consists of an unusual 9-ring pore, which runs parallel to the *a* axis and has dimensions of approximately 4.0 × 4.9 Å (assuming that the van der Waals diameter of the oxygen atom is 2.7 Å); these dimensions are similar to those of some 10-ring-pore zeolites. The other sets of channels run parallel to the *b* and *c* axes, and have pore apertures of approximately 4.8 × 5.1 and 4.8 × 5.7 Å, respectively. They consist of 10-ring systems that are similar to those seen in ZSM-5-type materials. The 9- and 10-ring channels are intercrossed

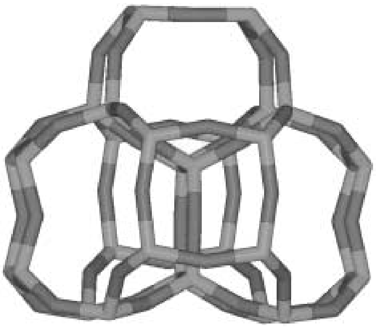

Figure 2. Characteristic building block of the ITQ-13 structure.

---

[*] Prof. A. Corma, M. Puche, Dr. F. Rey
Instituto de Tecnología Química (UPV-CSIC)
Universidad Politécnica de Valencia
Avenida Los Naranjos s/n, 46022 Valencia (Spain)
Fax: (+34) 96-3877809
E-mail: acorma@itq.upv.es

Dr. G. Sankar
Davy-Faraday Research Laboratory
The Royal Institution of Great Britain
21 Albemarle Street, London W1X 4BS (UK)

Dr. S. J. Teat
CLRL, Daresbury Laboratory
Daresbury, Warrington, Cheshire, WA4 4AD (UK)

[**] We thank Spanish CICYT (projects MAT 2000–1392 and MAT 2000-1167-C02-01) for financial support. A.C., M.P., and F.R acknowledge EXXON-Mobil for valuable support. G.S. and S.J.T thank the EPSRC for financial support. Also, the CRLC Daresbury Laboratory is gratefully acknowledged for their beam-time allocation.

Supporting information for this article is available on the WWW under http://www.angewandte.org or from the author.

throughout the material; this is the only zeolite reported to date that possesses 9- and 10-ring channels.

The unique aspects of the structure may be described more conveniently by considering the tertiary building block shown in Figure 2. It is interesting to note this subunit is related to the characteristic tertiary building block of the ITQ-21 zeolite,[6] which consists of a [$4^6 6^{12}$] cage with a 4-ring in its interior. In ITQ-13, however, one of the external 4-rings is absent, as illustrated in Figure 3.

The ITQ-13 subunits stack in the *a* direction through the connection of adjacent 4-rings of neighboring tertiary building blocks. The linkage yields a double 4-ring (D4R), which also appear in ITQ-21. The two neighboring tertiary building blocks in ITQ-13 also share a common 4-ring in the *b* direction. The presence of these fused 4-rings effectively results in a reduction in the pore opening from the 12-ring in ITQ-21 to a 9-ring in ITQ-13, and also decreases the symmetry within the *bc* plane. The topological analogies between zeolites ITQ-13 and ITQ-21 are more clearly shown in Figure 4.

The stacking sequence of the layers in the ITQ-13 structure, viewed along the *c* axis, is depicted in Figure 5. The framework is formed by an ABAB stacking sequence, which occurs through shifting the second layer by ±*b*/2, with respect to its neighboring layer. This particular connectivity gives rise to 9-ring channels that intersect the 10-ring pores aligned parallel to the *a* and *b* axes. In addition, the ±*b*/2 shift of the second layer produces the observed sinuosity of the channel running along the *c* axis. The staggered arrangements of D4Rs blocks the otherwise uninterrupted 10-ring channels parallel to the *c* axis. As a result, cylindrical cavities are formed with an approximate length and width of 15.5 and 5.3 Å, respectively. It is in these cavities where the hexamethonium structure-directing agent (SDA) is located, as illustrated in Figure 6. The long axes of the hexamethonium ions lie parallel to the *c* axis, but in a zigzag fashion that forms the sinusoidal 10-ring channels located along that crystallographic axis. Meanwhile, interactions between the charged alkyltrimethylammonium groups open the perpendicular 10-ring channel along the *b* axis.

Fluoride ions were located in two different crystallographic positions. One set are located in the center of the small D4R cages (two D4Rs per unit cell). However, since the two occluded hexamethonium dications give four positive charges per unit cell, only half of this charge is compensated by the fluoride ions in the D4R cages. The remaining fluoride

Table 1: Chemical composition of ITQ-13.

	Content [wt%]		X/N ratio	
	Experimental	Calculated[a]	Experimental	Calculated[a]
C	7.9	7.3	5.8	6.0
N	1.6	1.4	1.0	1.0
H	1.7	1.9	15.2	15.0
F	2.1	1.9	1.0	1.0
SiO_2	83.5[b]	85.9	12.2	14

[a] Values calculated for the following unit cell composition [$\{SiO_2\}_{56}\{[(CH_3)_3N(CH_2)_6N(CH_3)_3]^{2+}[F^-]_2\}_2$]$\cdot 4\,H_2O$. [b] Determined from thermogravimetic analysis.

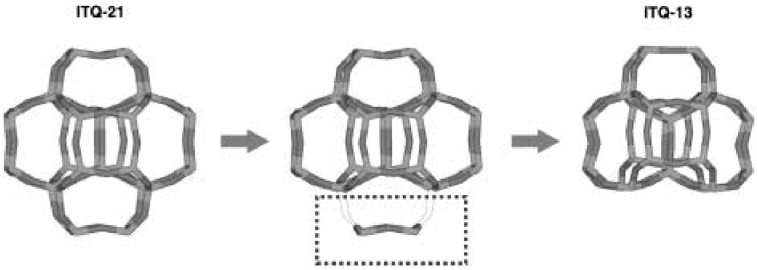

Figure 3. Relationship between the characteristic building blocks of the ITQ-13 and ITQ-21 zeolites.

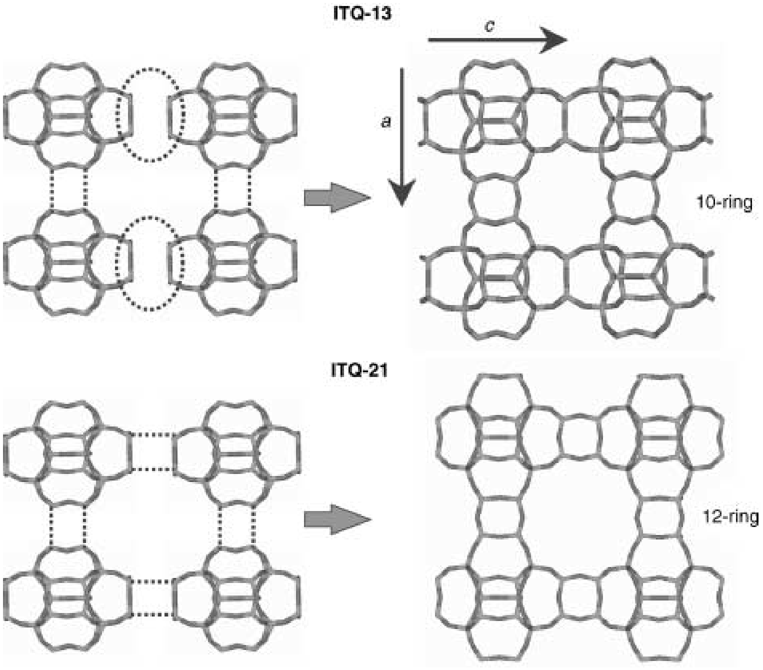

Figure 4. The building-block packing in the ITQ-13 structure normal to the *c* axis, compared to that of ITQ-21.

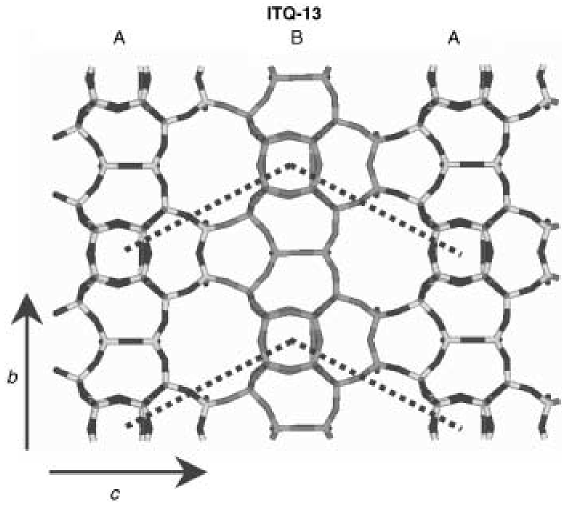

Figure 5. Stacking sequence of the characteristic layers of ITQ-13 along the *c* axis.

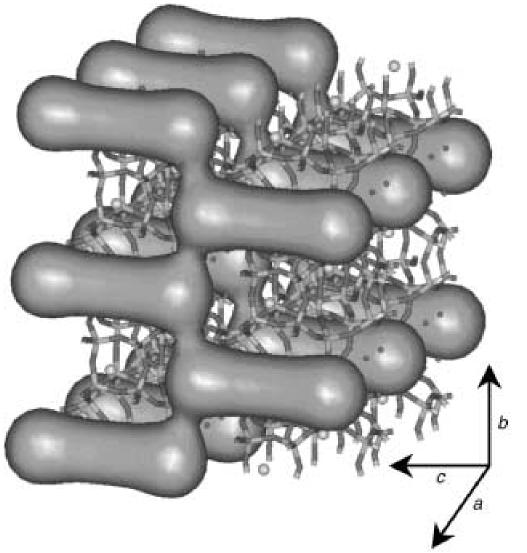

Figure 6. Idealised view of the location of the occluded hexamethonium cations that fill the pores of the ITQ-13 zeolite.

ions are located inside the $[4^15^26^2]$ cages; the smallest remaining cages within the ITQ-13 structure. The fluoride ions positioned at the center of the D4R cages are responsible for the observed ^{19}F MAS NMR signal at $\delta = -38$ ppm,[7] while the other resonance at $\delta = -66$ ppm can be attributed to those within the small $[4^15^26^2]$ cages,[8] with approximately the expected intensity ratio observed between the two signals.

The extra fluoride ions compensate for the charge of the organic dications located between the D4R units, and yields a final unit-cell composition of $[\{SiO_2\}_{56}\{[(CH_3)_3N(CH_2)_6N(CH_3)_3]^{2+}[F^-]_2\}_2]\cdot 4\,H_2O$, which is in good agreement with the experimental chemical analysis reported in Table 1.

We have previously reported other zeolites that contain D4R units as secondary building blocks.[6,9,10] The presence of D4R cages in the structure of ITQ-13 suggested that adding Ge to the synthesis gel should facilitate the formation of such D4R cages by aiding the nucleation process and, therefore, accelerating the crystallization rate of the zeolite. This phenomenon has been observed for ITQ-13; the synthesis time decreases when Ge was introduced to the synthesis gel. It should be noted, however, that for synthesis gels having a Si/Ge ratio lower than 5, ITQ-17, with the BEC structure,[10,11] starts to compete.

More importantly, we have succeeded in incorporating trivalent cations (B and Al) at framework positions. The ^{27}Al MAS NMR spectrum of an Al-containing ITQ-13 zeolite indicates the presence of tetrahedrally coordinated Al ions, which produce a resonance at $\delta = -52$ ppm. The IR spectrum of a calcined Al-ITQ-13 sample shows bands at 3614 and 3573 cm^{-1} that indicate the presence of hydroxyl groups; these bands disappear upon the adsorption of pyridine. Another distinct band at 1545 cm^{-1}, which results from protonated pyridine, indicates the presence of acid sites in this material.

In conclusion, the structure of ITQ-13 has been determined. The pore topology of this zeolite is unique, with a 9-ring channel system along the *a* axis, and 10-ring channel systems parallel to the *b* and *c* axes. Acid sites can be introduced into the structure, which opens the possibility for use in acid catalysis. Additionally, X-ray microdiffraction techniques have been used to solve the structure of ITQ-13 materials, and precisely locate the organic SDA and the corresponding fluoride ions.

Experimental Section

Synthesis: The synthesis protocol reported in example 1 of reference [13] was modified to maximize the average crystal size of ITQ-13, so that crystals large enough for single-crystal X-ray diffraction techniques were available.

The synthesis gel was prepared by hydrolyzing tetraethyl orthosilicate (31.20 g, 150 mmol) in an ethanolic solution (0.527 M) of hexamethonium dihydroxide ($HM(OH)_2$, 79.63 g, 42 mmol) with continuous stirring until all the ethanol had completely evaporated. Then, a 49 wt% aqueous solution of HF (3.495 g, 84 mmol) was introduced and water was added to give a water/silica ratio of 7. The final gel composition had the following molar composition:

$SiO_2 : 0.28\,HM(OH)_2 : 0.56\,HF : 7\,H_2O$.

Finally, the gel was autoclaved at 135 °C for 24 days. The solid was recovered by filtration, washed repeatedly with distilled water and acetone, then dried overnight at 80 °C. The occluded organic species were isolated by calcination in air at 550 °C.

The chemical composition of the as-prepared ITQ-13 zeolite is given in Table 1; the occluded organic cation remains intact after hydrothermal treatment and fully compensates the charge of the fluoride ions.

Synthesis of the Al-containing ITQ-13 was achieved by exchange of the boron ions[12] in B-ITQ-13, which was prepared by introducing the appropriate amount of boric acid to reach the following molar composition of the gel:

$SiO_2 : 0.01\,B_2O_3 : 0.29\,R(OH)_2 : 0.64\,HF : 7\,H_2O$

4 wt% SiO_2 was added to purely siliceous ITQ-13 as seeds for the acceleration of crystallization. The resulting gel was autoclaved at 135 °C for 24 days, and the as-prepared B-ITQ-13 was recovered by filtration, repeatedly washed with distilled water, and dried at 80 °C for 12 h.

As-prepared B-ITQ-13 was calcined at 550 °C for 6 h in air. The sample was then treated with an aqueous solution of aluminum nitrate (8 wt%) at 140 °C for 72 h under hydrothermal conditions, and Al-ITQ-13 was recovered by filtration, repeatedly washed with distilled water, and dried at 80 °C for 12 h.

X-ray diffraction: Powder diffraction data were collected on an X'Pert diffractometer with Bragg–Brentano geometry provided with a secondary graphite monochromator. Intensity data were obtained with a variable-divergence slit using $Cu_{K\alpha1,2}$ radiation ($\lambda = 1.5406$, 1.5444 Å). The tube settings were 45 kV and 40 mA and the step scan size and time were 0.02° and 10 s, respectively.

Microcrystal X-ray diffraction data were obtained at Station 9.8 of the CLRC Daresbury Laboratory Synchrotron Radiation Source equipped with a Bruker AXS diffractometer with a CCD detector. X-ray radiation was selected at $\lambda = 0.6942$ Å by using a Si(111) monochromator and vertically focused by a cylindrically bent Pd-coated zerodur mirror. The single-crystal data were collected at low temperature ($T = 150$ K). The structure was solved and refined on F^2 using published programs and techniques[14] to converge at $R1 = 0.0800$ (for reflections with $I > 2\sigma(I)$), $wR2 = 0.2081$, and $S = 1.014$ for 280 parameters. Maximum residual electron density = 2.87 e Å^{-3}. The template molecule was modeled isotropically with geometrical and displacement parameter restraints; hydrogen atoms were placed in calculated positions and refined using a riding model. The framework atoms were modeled anisotropically with displacement parameter restraints. The Si7–F2 bond length was constrained to be that obtained from NMR data.[15]

CCDC-196854 contains the supplementary crystallographic data for this paper. These data can be obtained free of charge via www.ccdc.cam.ac.uk/conts/retrieving.html (or from the Cambridge Crystallographic Data Centre, 12 Union Road, Cambridge CB2 1EZ, UK; fax: (+44) 1223-336-033; or deposit@ccdc.cam.ac.uk).

Solid-state NMR: Spectra were recorded using magic-angle spinning (MAS) techniques at room temperature. ^{19}F spectra were measured in a Bruker Av-400 spectrometer at 376.8 MHz in 2.5 mm diameter zirconia rotors at a spinning rate of 30 kHz. The spectra were collected using 3 μs pulses, which correspond to a magnetization flip angle of $\pi/2$ rad and a recycle delay of 100 s, to ensure the complete recovery of the magnetization; the spectra were referenced to $CFCl_3$. Solid-state ^{27}Al MAS NMR spectra were recorded on a Varian Unity VXR-400 WB spectrometer at 104.2 MHz, with a $\pi/18$ rad pulse length, a recycle delay of 0.5 s, and spinning rate of 7 kHz.

Received: November 11, 2002 [Z50514]

Keywords: heterogeneous catalysis · microporous materials · structure elucidation · X-ray diffraction · zeolites

---

[1] C. Baerlocher, W. M. Meier, D. H. Olson, *Atlas of zeolite framework types*, 5th rev. ed., Elsevier, Amsterdam, **2001**. Also in http://www.iza-structure.org/.
[2] A. Corma, *Chem. Rev.* **1995**, *95*, 559.
[3] a) P. B. Venuto, *Microporous Mater.* **1994**, *2*, 297; b) P. B. Venuto, *Stud. Surf. Sci. Catal.* **1997**, *105*, 811.
[4] N. Y. Chen, W. E. Garwood, F. G. Dwyer, *Shape Selective Catalysts in Industrial Applications*, 2nd rev. ed., Marcel Dekker, New York, **1996**.
[5] G. Sastre, J. D. Gale, *Microporous Mesoporous Mater.* **2001**, *43*, 27.
[6] A. Corma, M. J. Díaz-Cabañas, J. Martínez-Triguero, F. Rey, J. Rius, *Nature* **2002**, *418*, 514.
[7] a) P. Caullet, J. L. Guth, J. Hazm, J. M. Lamblin, *Eur. J. Solid State Inorg. Chem.* **1991**, *28*, 359; b) J. L. Guth, H. Kessler, P. Caullet, J. Hazm, A. Merrouche, J. Patarin in *Proc. 9th Inter. Zeolite Conf., Vol. I* (Eds.: R. Von Ballmoos, J. B. Higgins, M. M. J. Treacy) Butterworth-Heinemann, London, **1993**, p. 215.
[8] C. A. Fyfe, D. H. Brouwer, A. R. Lewis, J. M. Chézeau, *J. Am. Chem. Soc.* **2001**, *123*, 6882.
[9] a) A. Corma, M. J. Díaz-Cabañas, V. Fornés, *Angew. Chem.* **2000**, *112*, 2436; *Angew. Chem. Int. Ed.* **2000**, *39*, 2346; b) T. Blasco, A. Corma, M. J. Diaz-Cabañas, F. Rey, J. A. Vidal-Moya, C. M. Zicovich-Wilson, *J. Phys. Chem. B* **2002**, *106*, 2637.
[10] a) A. Corma, M. T. Navarro, F. Rey, J. Rius, S. Valencia, *Angew. Chem.* **2001**, *113*, 2337; *Angew. Chem. Int. Ed.* **2001**, *40*, 2277; b) A. Corma, M. T. Navarro, F. Rey, S. Valencia, *Chem. Commun.* **2001**, 1486.
[11] a) C. Baerlocher, W. M. Meier, D. H. Olson, *Atlas of zeolite framework types*, 5th rev. ed., Elsevier, Amsterdam, **2001**). Also in http://www.iza-structure.org/. b) T. Conradsson, M. S. Dadachov, X. D. Zou, *Microporous Mesoporous Mater.* **2000**, *41*, 183.
[12] T. Boix, M. Pucha, M. A. Camblor, A. Corma, U.S. Pat. 6,471,941 B1 **2000**.
[13] C. Y. Chen, S. I. Zones, *Stud. Surf. Sci. Catal.* **2001**, *135*, 1710.
[14] a) G. M. Shelrick, SHELXS and SHELXL programs. University of Göttingen, Germany, **1997**; b) W. Clegg, M. R. J. Elsegood, S. J. Teat, C. Redshaw, V. C. Gibson, *J. Chem. Soc. Dalton Trans.* **1998**, 3037.
[15] I. Bull, L. A. Villaescusa, S. J. Teat, M. A. Camblor, P. A. Wright, P. Lightfoot, R. E. Morris, *J. Am. Chem. Soc.* **2000**, *122*, 7128.

Berichtigungen

In der Zuschrift „A Zeolite Structure (ITQ-13) with Three Sets of Medium-Pore Crossing Channels Formed by 9- and 10-Rings“ von **A. Corma et al.** in *Angew. Chem.* **2003**, *115*, 1188–1191; *Angew. Chem. Int. Ed.* **2003**, *42*, 1156–1159, hätte schon am Anfang des Manuskripts deutlich gemacht werden sollen, dass die Synthese des ITQ-13-Materials erstmals in einem 2002 veröffentlichten Patent beschrieben wurde (T. Boix, M. Puche, M. A. Camblor, A. Corma, US Patent 6471941 B1, **2002**; Lit. [12] im Manuskript). Weiterhin wurde wegen eines redaktionellen Versehens der Literaturverweis zu diesem Patent in der *Experimental Section* falsch eingetragen: Statt Lit. [13] sollte es dort richtigerweise Lit. [12] lauten und umgekehrt.

Wir bitten unsere Leser und die Autoren des genannten Patents um Entschuldigung.

Avelino Corma
Korrespondenzautor

Peter Gölitz
Chefredakteur

In der Zuschrift von **S. Shimada und M. Tanaka et al.** in *Angew. Chem.* **2003**, *115*, 1889–1892, wurde auf S. 1889 eine falsche Formel abgedruckt. Die korrekte Formel ist hier gezeigt. Des Weiteren lautet die E-mail-Adresse von Professor Tanaka: m.tanaka@res.titech.ac.jp.

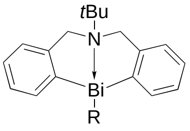

3a – 3g

3a: R = Ph
3b: R = 3,5-$(CF_3)_2C_6H_3$-
3c: R = 3,4-$(CH_2O_2)C_6H_3$-
3d: R = 2,4,6-$(MeO)_3C_6H_2$-
3e: R = CH_2=C(Me)-
3f: R = Br
3g: R = Cl

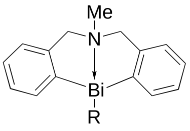

4

In der Übersetzung des IUPAC-Glossars zur Theoretischen Organischen Chemie (*Angew. Chem.* **2003**, *115*, 2248–2294) sind der Name und der Wert einer Naturkonstante fehlerhaft: Es handelt sich um die Avogadro-Konstante (nicht Avagadro), deren Wert $6.0221367(36)\times10^{23}$ mol^{-1} (nicht $6.00221367(36)\times10^{23}$ mol^{-1}) ist.